J Comput Aided Mol Des (2010) 24:829–841
DOI 10.1007/s10822-010-9377-x

Mechanisms of amphipathic helical peptide denaturation by guanidinium chloride and urea: a molecular dynamics simulation study

Faramarz Mehrnejad · Mahmoud Khadem-Maaref · Mohammad Mehdi Ghahremanpour · Farahnoosh Doustdar

Received: 6 May 2010 / Accepted: 29 July 2010 / Published online: 10 August 2010

Abstract Urea and GdmCl are widely used to denature proteins at high concentrations. Here, we used MD simulations to study the denaturation mechanisms of helical peptide in different concentrations of GdmCl and urea. It was found that the helical structure of the peptide in water simulation is disappeared after 5 ns while the helicity of the peptide is disappeared after 70 ns in 2 M urea and 25 ns in 1 M GdmCl. Surprisingly, this result shows that the helical structure in low concentration of denaturants is remained more with respect to that solvated in water. The present work strongly suggests that urea interact more preferentially to non-polar and aromatic side chains in 2 M urea; therefore, hydrophobic residues are in more favorable environment in 2 M urea. Our results also reveal that the hydrogen bonds between urea and the backbone is the dominant mechanism by which the peptide is destabilized in high concentration of urea. In 1 M and 2 M GdmCl, GdmCl molecules tend to engage in transient stacking interactions with aromatics and hydrophobic planar side chains that lead to displacement of water from the hydration surface, providing more favorable environment for them. This shows that accumulation of GdmCl around hydrophobic surfaces in 1 M and 2 M GdmCl solutions prevents proper solvation of the peptide at the beginning. In high GdmCl concentrations, water solvate the peptide better than 1 M and 2 M GdmCl. Therefore, our results strongly suggest that hydrogen bonds between water and the peptide are important factors in the destabilization of peptide in GdmCl solutions.

Keywords Osmolytes · Alpha helical peptide · Urea · Guanidinium chloride · Hydrogen bond · Hydrophobic interaction

Introduction

During the course of several billion years of evolution, polypeptides have adapted to their aqueous environments by exploiting the physical properties of water. Therefore, the solvent and co solvent play a central role in the non-covalent interactions responsible for the unique three-dimensional structures of native proteins. The intramolecular or intermolecular hydrogen bonds and the hydrophobic effects provide the main driving force for correct folding of proteins [1]. The stability and instability of proteins, conferred by numerous but non-covalent interactions, is marginal [2]. A fundamental understanding of protein folding and stability, including the mechanism of action of co solvents, must be based on the studies of the structure, solvation and energetic of nonnative proteins at a level of detail comparable with what has been achieved for native polypeptides [3]. The denaturing osmolytes such as guanidinium chloride (GdmCl) and urea have been employed in unfolding/refolding experiments. In contrast, 2, 2, 2 trifluoroethanol (TFE) is another osmolyte that has been used to study polypeptides in solutions because

Electronic supplementary material The online version of this article (doi:10.1007/s10822-010-9377-x) contains supplementary material, which is available to authorized users.

F. Mehrnejad (✉) · M. M. Ghahremanpour
Department of Cellular and Molecular Biology, Faculty of Science, Azarbaijan University of Tarbiat Moallem, P.O. Box 53714-161, Tabriz, Iran
e-mail: mehrnejad@azaruniv.edu

M. Khadem-Maaref
Department of Physics, Faculty of Science, Azad University of Bonab, Bonab, Iran

F. Doustdar
Department of Microbiology, Faculty of Medicine, Shahid Beheshti University of Medical Sciences, Tehran, Iran

experimental investigations show that alpha helical peptides are readily stabilized in the less polar environment of TFE/water mixtures [4–8]. Unfolding by urea and GdmCl is a standard method to investigate the protein and peptide stability and to study the mechanisms of protein folding [9]. Although GdmCl and urea are widely used as denaturant agents, it is not clear by which molecular mechanisms they denature proteins. There are three models for protein denaturation by urea and GdmCl. In the first model, these molecules interact directly with the protein, particularly by hydrogen bonding to the polar groups competing with intramolecular hydrogen bonding. In the second model, the effects are indirect, that is, GdmCl and urea change the hydrogen bond network of the solvent around hydrophobic groups, providing a better solvation environment and decreasing the hydrophobic effect. In the third model, there is a combination of direct and indirect effects [10–12]. Overall, previous molecular dynamics simulations support the role of both of these effects in urea and GdmCl denaturation [13–20]. To study the interactions of osmolytes with the surface of a folded peptide, we have performed all-atom molecular dynamics simulations of helical peptide, magainin2 (PDB ID: 2mag), in different concentrations of GdmCl and urea. Magainin 2 is a 23-residue long, amphipathic, alpha helical antimicrobial peptide that is secreted by the skin of the African frog *Xenopus laevis*. The sequence of the peptide is as follow: GIGKFLHSAKKFGKAFVGEIMNS. Previous studies have shown that magainin adopts a very similar alpha helical structure in different environments [21]. In pure water, Magainin behaves as a random coil [7].

MD simulations can provide valuable information about the various stages of peptide-solvent interactions. Previous molecular dynamics studies have shown the effect of solvent, co solvent and membrane on the stability of the alpha helical structure [7, 21–24]. The main goal of our work is to study the interactions of the helical model peptide with urea and GdmCl molecules. The general belief is that for a stable peptide one hardly can see the effect of denaturant at short time scale. Since marginally stable peptides are good candidate to investigate organic solvent effects on peptide stability, we used magainin. These simulations can help us to investigate the molecular level and the structural effects of different concentrations of GdmCl and urea on this model peptide. The simulations in aqueous GdmCl and urea solutions are anyway compared with simulations performed in pure water and TFE/water mixture to discriminate the net effect of denaturant.

Computational methods

All MD simulations were performed using the GROMACS [25, 26] simulation package, versions 3.3 and 3.3.1. The GROMOS96 force field [27] as implemented in the GROMACS was used [25, 26, 28].

Molecular dynamics simulation setup

The starting conformation for the simulations of the peptide was obtained from the protein databank (PDB ID: 2mag) [21]. The peptide was solvated with SPC water [29], a mixture of urea [30], a mixture of GdmCl [17], and a mixture of TFE [31] and SPC water and placed in a cubic box large enough to contain the peptide and 1 nm of solvent on all sides. For the simulations with counter-ions, Cl counter-ions were added to neutralize the total charge of the systems. Lennard-Jones interactions were calculated with a 0.9/1.4-nm twin-range cut off. The short-range electrostatic interactions were calculated to1.0 nm, and Particle Mesh Ewald algorithm was used for the long-range interactions [32]. All simulations were performed in the NpT-ensemble using Berendsen-type temperature-coupling with a coupling coefficient of $\tau_T = 0.1$ ps and Berendsen-type pressure-coupling at 1 bar with coupling coefficient of $\tau_P = 0.1$ ps [33]. Simulations were run with 2-fs time steps. Bond length was constrained using the LINCS algorithm [34]. All atoms were given an initial velocity obtained from a Maxwellian distribution at the desired initial temperature. All of the simulations, starting from average NMR structure, were equilibrated by 100 ps of MD with position restraints on the peptide to allow for the relaxation of the solvent molecules. For each of the nine systems, three independent trajectories were obtained. The production runs at the constant temperature and pressure conditions, after equilibration, were 40 ns long. A summary of the simulations is listed in Table 1.

Table 1 Summary of the MD simulations

Peptide	Solvent	No. of water molecules	No. of denaturant molecules	T(K)	Duration (ns)
Magainin	Water	3,550	–	300	40
Magainin	TFE/water	2,384	468	300	40
Magainin[a]	Urea 2 M	3,365	175	300	40
Magainin	Urea 4 M	2,958	290	300	40
Magainin	Urea 8 M	2,572	569	300	40
Magainin	GdmCl 1 M	2,869	57	300	40
Magainin	GdmCl 2 M	2,741	111	300	40
Magainin	GdmCl 4 M	2,410	179	300	40
Magainin	GdmCl 6 M	2,350	405	300	40

[a] The simulation time is 70 ns (supporting information)

Contact coefficient

To illustrate the frequency of interactions between the amino acids and urea in details, we have calculated the contact coefficient C_{DW} for a particular amino acid X:

$$C_{DWX} = \frac{N_{X-D} M_W}{N_{X-W} M_D} \quad (1)$$

where N_{X-W} and N_{X-D} are the numbers of atomic contacts of amino acid X with water and denaturant molecules, respectively. Here, we defined in contact if they are closer then 0.35 nm. To normalize C_{DW} values, the total numbers of denaturant atoms (M_D) and water atoms (M_W) were used. The contact coefficient of $C_{DW} = 1.0$ shows that the residue X has no preferential interaction with either denaturant or water. Values below 1.0 indicate preferential interaction with water; values above 1.0 show preferential interaction with denaturant [18, 35].

Potential of mean force

Potential of mean force (PMF) was calculated between the solutes using

$$W_{\beta(r)} = -k_B T Ln(g(r)) \quad (2)$$

Where $W_{\beta(r)}$ ($\beta = C_\beta$ of hydrophobic residues) is the PMF, k_B is the Boltzman constant, T is the simulation temperature and $g(r)$ is the radial distribution function (RDF) between the solutes [1, 36].

Analysis

The analyses were performed on the ensemble of system configurations extracted at 0.5 ps time intervals from the simulations. Least-squares fitting of atomic coordinate for the calculation of structural properties of the peptide such as the atom positional root-mean-square deviation or difference (RMSD) were based on the peptide atoms (C_{alpha}) of all residues. The hydrogen bonds were calculated using a geometric criterion. A hydrogen bond was defined by a minimum donor-hydrogen-acceptor angle of 135° and a maximum hydrogen-acceptor distance of 0.25 nm. The secondary structure was classified using DSSP [37].

Results

Helix stability

We first analyzed the structural dynamics and the stability of the folded peptide as well as its peptide-solvent interactions in water, in TFE/water, and in the different concentration of GdmCl and urea. In Fig. 1, the C_{alpha} root mean square deviation (RMSD) with respect to the initial structure for the peptide in all environments as a function of time is reported. The peptide remains practically unchanged along TFE/water simulation, with RMSD average below 0.3 nm. As found previously [7, 24], magainin is unstable in water simulation and in this work the RMSD rises almost continuously over the first 5 ns (Fig. 1). In 2 M urea and TFE/water mixture, the RMSD reaches a value of $\sim$ 0.31 nm within the first 9 ns (Fig. 1a). This value is similar to that obtained in our previous study [7]. After 10 ns, the RMSD in 2 M urea overcomes 0.5 nm and unfolding is observed (Fig. 1a). In 4 M urea, the RMSD rises almost continuously over the first 4.5 ns, to a peak of 0.41 nm (Fig. 1a). Magainin begins to unfold gradually, from the first 3 ns of the 8 M urea simulation (Fig. 1a). In the first 20 ns, the curves corresponding to the simulations in 1 M and 2 M GdmCl are similar 0.43 nm (Fig. 1b). After 25 ns, the RMSDs reach a value in excess of 0.6 nm (Fig. 1b).The peptide begins to gradually unfold, from the first picoseconds of the 4 and 6 M GdmCl simulations (Fig. 1b). An important observation indicates that in the all-unfolding simulations in urea, GdmCl and water, the alpha helix is destabilized,very rapidly, in water and high concentration of urea and GdmCl while, in 2 M urea, the unfolding is observed after 10 ns and the peptide begins to gradually unfolds from 20 ns in the 1 and 2 M GdmCl.

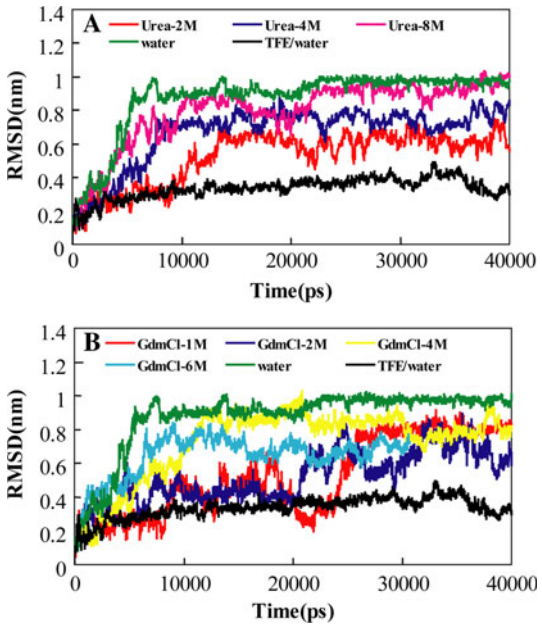

Fig. 1 The C_{alpha} root mean square deviation (RMSD) of the peptide with respect to the initial NMR structure for the simulations

Figure 2 shows variations in the secondary structure of the peptide during the simulations, as defined by dictionary of secondary structure of proteins (DSSP). In all cases, the peptide secondary structure deteriorates with time from an

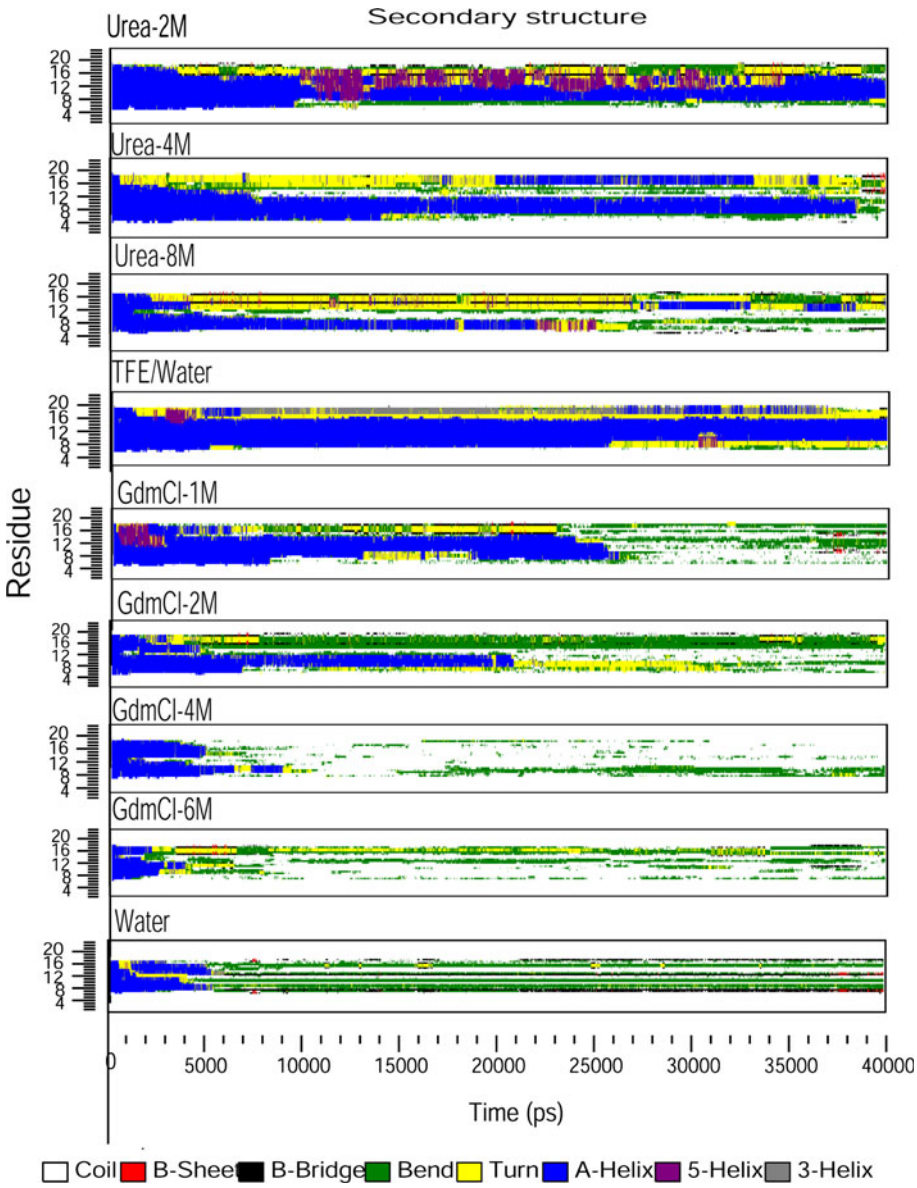

Fig. 2 Summery of the secondary structure identified (according to the Kabsch and Sander procedure) in the water, TFE/water, aqueous urea and guanidinium chloride solutions

initial helical structure. For magainin in TFE/water and 2 M urea, the largely alpha helical conformation of the peptide is maintained throughout the 9 ns duration of the simulation and there are occasional local deviations from alpha helicity in the C-terminal part of the molecule (Fig. 2). In 2 M urea, the alpha helicity of magainin decreases at C-terminus of the peptide starting at 10 ns. In the end of 2 M urea simulation, residues 8-16 remain in an alpha helical conformation (Fig. 2). In 4 M urea, the helicity of peptide deteriorates in the C-terminus of the molecule starting at 1.5 ns and completely unfolds at the end of simulation (Fig. 2). The peptide begins to unfold completely from the first nanosecond of the 8 M urea simulation. In water, the alpha helicity of peptide decreases at the C-terminus of the molecule starting at 2 ns and reaching its maximum extent at 3 ns. In 1 M GdmCl, the largely alpha helical structure of the peptide is remained throughout the 9 ns duration of the simulation. After 9 ns, the helicity of magainin decreases in the C-terminal and N-terminal parts of peptide, and at 25 ns, the helicity of peptide is completely disappeared (Fig. 2). The peptide begins to unfold completely from the first nanosecond of the 4 M and 6 M GdmCl simulations (Fig. 2).

The time average of the alpha helicity at early and late stages of the MD simulations is reported in Fig. 3. If we consider as threshold an alpha helicity value of 20%, the helix are comprised between residues 5–16 for the TFE simulation, residues 5–15 for 2 M urea simulation, residues 5–10 for 4 M urea simulation, and residues 13–15 for 8 M urea simulation (Fig. 3—last 5 ns). The original helicity is kept until 16 in TFE/water simulation and 15 in 2 M urea simulations (Fig. 3—last 5 ns).

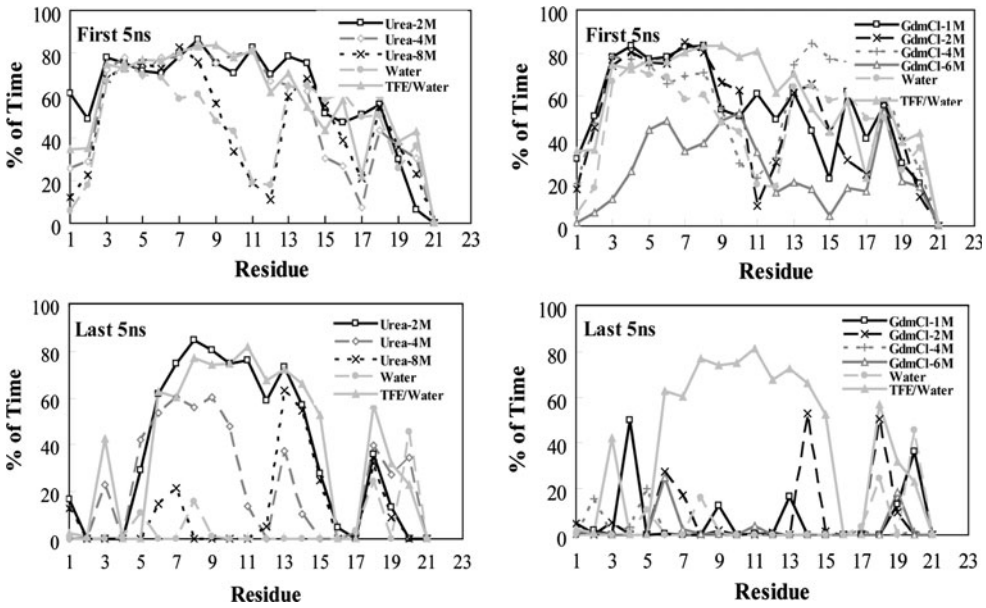

Fig. 3 The helicity per residue of magainin in the water, TFE/water, aqueous urea and guanidinium chloride solutions the early and the last stages of the simulations, First 5 ns, Last 5 ns

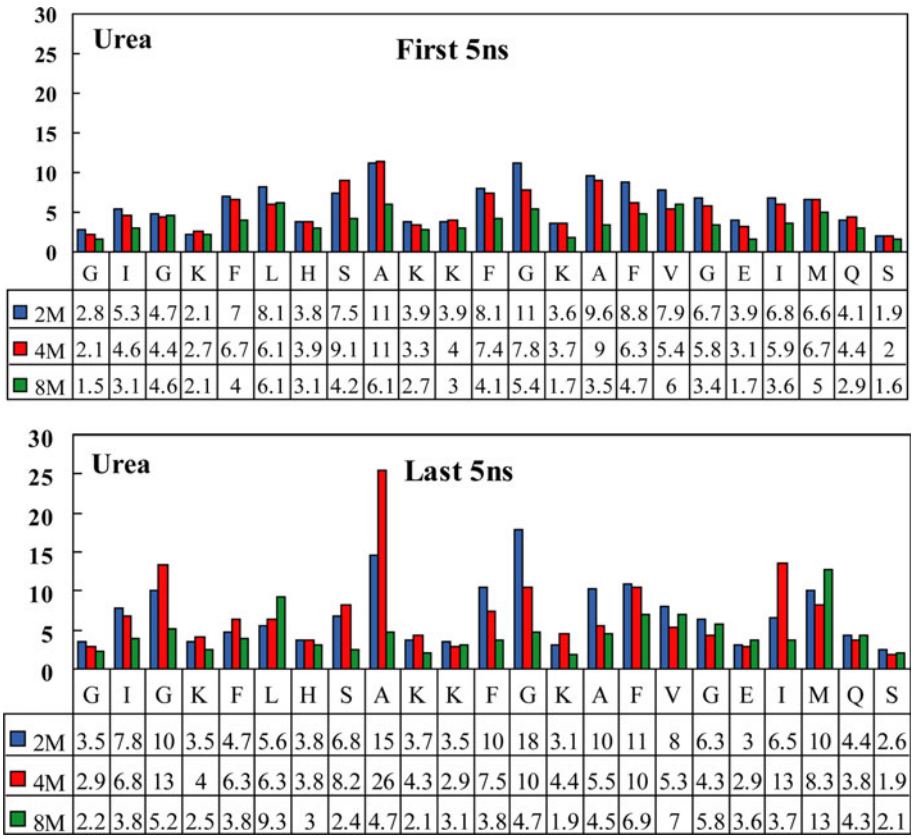

	G	I	G	K	F	L	H	S	A	K	K	F	G	K	A	F	V	G	E	I	M	Q	S
2M	2.8	5.3	4.7	2.1	7	8.1	3.8	7.5	11	3.9	3.9	8.1	11	3.6	9.6	8.8	7.9	6.7	3.9	6.8	6.6	4.1	1.9
4M	2.1	4.6	4.4	2.7	6.7	6.1	3.9	9.1	11	3.3	4	7.4	7.8	3.7	9	6.3	5.4	5.8	3.1	5.9	6.7	4.4	2
8M	1.5	3.1	4.6	2.1	4	6.1	3.1	4.2	6.1	2.7	3	4.1	5.4	1.7	3.5	4.7	6	3.4	1.7	3.6	5	2.9	1.6

	G	I	G	K	F	L	H	S	A	K	K	F	G	K	A	F	V	G	E	I	M	Q	S
2M	3.5	7.8	10	3.5	4.7	5.6	3.8	6.8	15	3.7	3.5	10	18	3.1	10	11	8	6.3	3	6.5	10	4.4	2.6
4M	2.9	6.8	13	4	6.3	6.3	3.8	8.2	26	4.3	2.9	7.5	10	4.4	5.5	10	5.3	4.3	2.9	13	8.3	3.8	1.9
8M	2.2	3.8	5.2	2.5	3.8	9.3	3	2.4	4.7	2.1	3.1	3.8	4.7	1.9	4.5	6.9	7	5.8	3.6	3.7	13	4.3	2.1

Fig. 4 Interaction coefficient C_{uw} for all residues in magainin: aqueous urea solutions

Contact coefficient

To identify distribution of solvent and co solvent molecules around the peptide in GdmCl and urea solutions, we focus on contact coefficient C_{DW} of each particular peptide residues. Fig. 4 shows the C_{UW} values for each residue type in the peptide, averaged over the MD simulations and over time. As shown in Fig. 4, C_{UW} is higher than 1, demonstrating favorable contacts with urea for all amino acids. Our results show that the urea molecules interact largely with aromatic and non-polar residues supported by previous studies [18, 19, 35]. The pronounced interactions with urea are seen for the aromatic rings of Phe^{5}, Phe^{12}, Phe^{16} and the aliphatic side chains of Ile^{2}, Ile^{20}, Leu^{6} and Ala^{9},

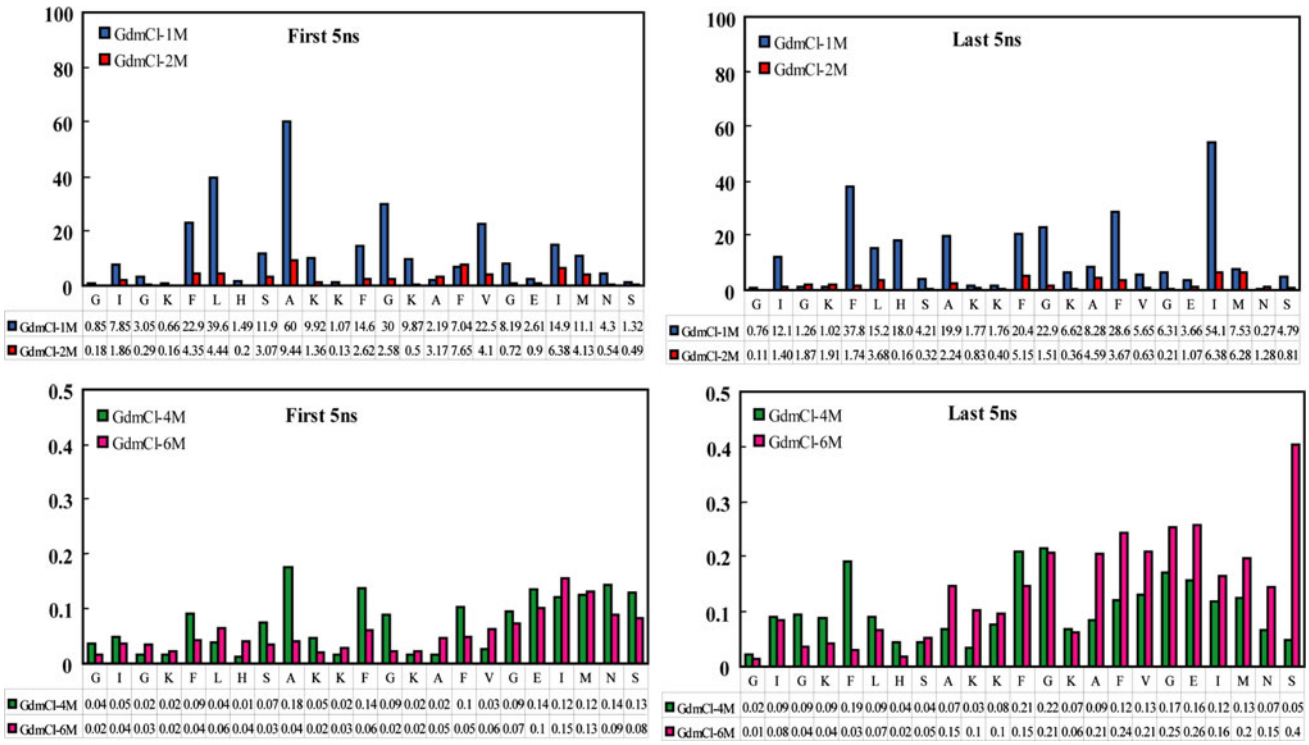

Fig. 5 Interaction coefficient C_{gw} for all residues in magainin: aqueous GdmCl solutions

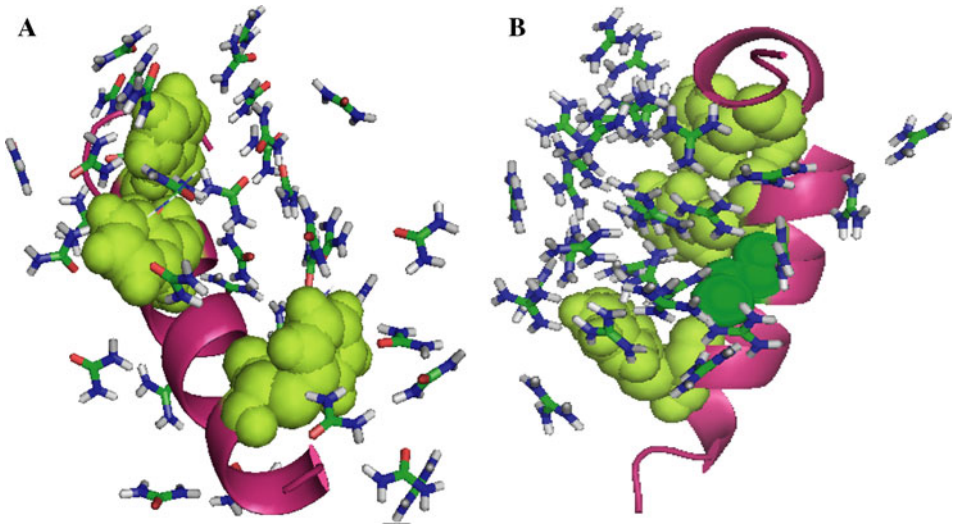

Fig. 6 Snapshots from the MD simulations showing urea and GdmCl within in 0.6 nm of residues Phe[5], Phe[12], and Phe [16] in urea 2 M (**a**) and GdmCl 1 M (**b**)

Ala [15]. As can be seen, low urea concentration has a preference over high urea solutions in binding to non-polar residues, indicating that in 2 M urea solution, urea molecules could penetrate to the hydrophobic surface of the peptide better than 4 M and 8 M urea solutions. Thus, non-polar residues might sense more favorable environment in low urea concentrations due to the accumulation of the urea molecules near the hydrophobic surfaces. The magainin has a hydrophobic surface made up aromatic and aliphatic side chains, allowing us to consider the interactions of GdmCl with hydrophobic regions normally buried in a folded protein (Fig. 6a). Contact coefficient analysis presented in Fig. 5 describes which residues of the peptide show contact preferences for GdmCl in different concentrations. As shown, GdmCl molecules preferentially bind to the hydrophobic residues, both aromatic and aliphatic side chains, in 1 M and 2 M GdmCl solutions. This result is in agreement with the experiment by Mason et al., [20] that GdmCl molecules accumulate near hydrophobic surface by weak stacking interactions with planar π-systems of

aromatics side chains. In contrast, approximately all residues of the magainin significantly contact to water molecules in 4 M and 6 M GdmCl, indicating better solvation of the peptide in higher GdmCl concentration in compare to lower concentration. Stacking interactions of GdmCl molecules, in solutions of 1 M and 2 M GdmCl, with hydrophobic surfaces of the magainin displacement of water from the hydration surface (Fig. 6b), providing more favorable environment for aromatic and aliphatic non-polar side chains.

Hydrogen bond

The analysis of the intramolecular backbone hydrogen bonds reflects the observations made in the conformational analysis of the simulations (see supporting information: Table 2). As can be seen, the hydrogen bonds characteristic for the alpha helical conformation are largely populated in TFE/water mixture and in 2 M urea simulation. In water, 8 M urea and 6 M GdmCl simulations, the alpha helical hydrogen bonds disappear in the peptide. Figures 7 and 8 show the total number of hydrogen bonds between the peptide and solvents over the course of the MD simulations. In the TFE/water simulation, the total number of hydrogen bonds between TFE with backbone and side chain increases while the total number of backbone-water and side chain-water hydrogen bonds decreases. The TFE/water simulation shows that the intramolecular backbone-backbone hydrogen bonds remain constant with time (Fig. 7). Surprisingly, our comparative MD simulations show that the total number of backbone-urea hydrogen bonds increases and the intramolecular backbone-backbone hydrogen bonds decrease partially with time in 2 M urea. As the concentration of urea increases, the number of

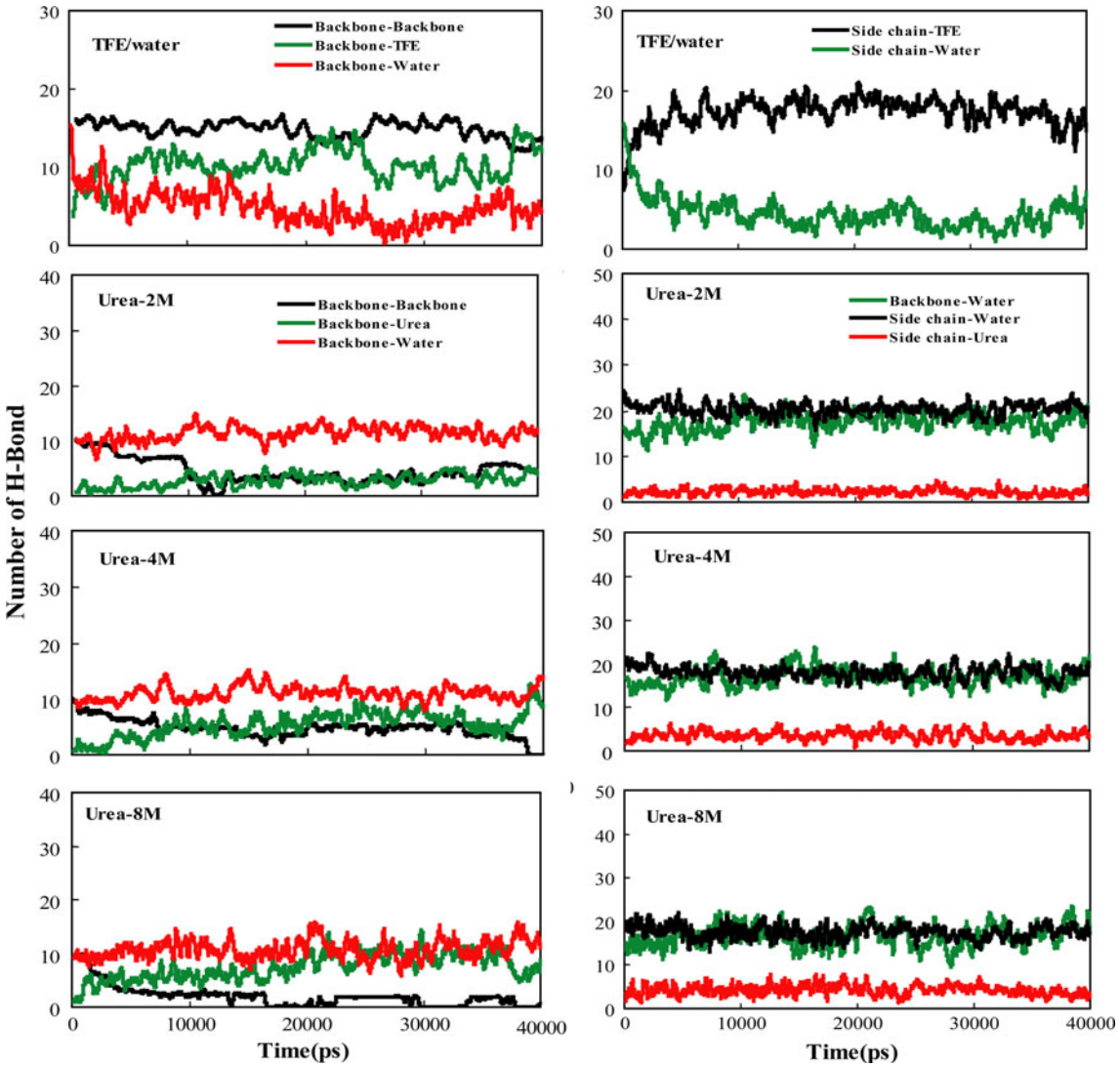

Fig. 7 The total number of hydrogen bonds between backbone–backbone, backbone–Urea, backbone–Sol, Side chain–Urea and side chain–Sol

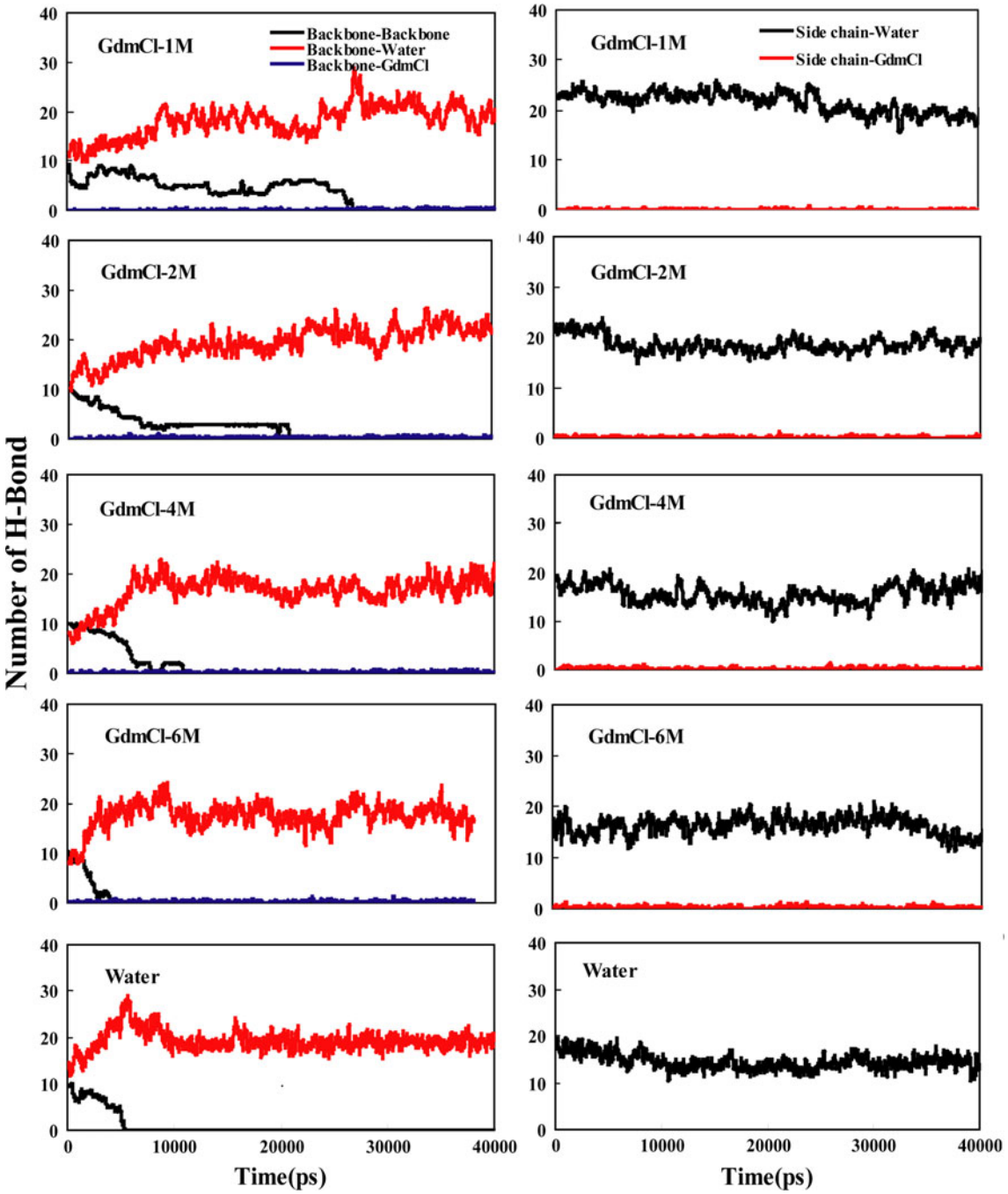

Fig. 8 The total number of hydrogen bonds between backbone–backbone, backbone–GdmCl, backbone–Sol, side chain–GdmCl and side chain–Sol

hydrogen bonds between backbone and urea increases most rapidly in 10 ns (Fig. 7). In contrast, the total number of backbone-water, side chain-urea and side chain-water hydrogen bonds remain constant in all concentration of urea (Fig. 7). These data suggest that the urea molecules attach themselves to the peptide, and the backbone-backbone hydrogen bonds are replaced by backbone-urea hydrogen bonds. Thus, the hydrogen bonds between the peptide and urea molecules are thought to stabilize the denatured state and lead to peptide denaturation. In water simulation, the total number of hydrogen bonds between the backbone with water increases and the intramolecular backbone-backbone hydrogen bonds decrease most rapidly and disappear after 5 ns. In 1 M and 2 M GdmCl simulations, the intramolecular backbone-backbone hydrogen bonds decrease with time and finally disappear while the total number of backbone-water and backbone-GdmCl hydrogen bonds increases (Fig. 8). In 4 M and 6 M

GdmCl, the intramolecular backbone-backbone hydrogen bonds decrease and disappear most rapidly and the total number of hydrogen bonds between the backbone with water and GdmCl increases during the simulation. After 3 ns and 8 ns the alpha helical structure disappears in 6 M and 4 M GdmCl, respectively (Fig. 8). During all the simulations, the number of hydrogen bonds between side chain with water and GdmCl is approximately constant (Fig. 8). The present work suggests that the number of hydrogen bonds between backbone with water and GdmCl increases with time but this increase is more prominent for water comparing GdmCl (Fig. 8).

Direct interaction between peptide and co solvents

To show the structural changes due to the interactions between osmolytes and peptide, we have calculated a number of atomic radial distribution functions to compare the strength of direct interactions between different atoms of the urea and GdmCl molecules and the backbone of peptide during the first and the last 5 ns of the simulation time. The magnitude of the first peak of the pair correlation functions between water oxygen and amide nitrogen is directly proportional to the GdmCl concentration (Fig. 9), suggesting of more preferentially binding of the water oxygen to the backbone protons in high GdmCl solutions that is consistent with the results of contact coefficient analysis. There are more ordered water molecules near the amide nitrogen in the last 5 ns than in the first 5 ns, indicative of better solvation of the backbone atoms with time (Fig. 9). The strength of the g (r) profile between the GdmCl nitrogen and the amide oxygen is higher compare to the g (r) magnitude between the water oxygen and the amide nitrogen particularly in low GdmCl solutions (Fig. 9). Thus, GdmCl interacts more strongly with the backbone than water, suggesting that accumulation of GdmCl around the backbone causes poor solvation of the peptide in low GdmCl aqueous solutions.

Both urea nitrogen and carbonyl oxygen can bind to the backbone carbonyl oxygen and the amide nitrogen, respectively. In all urea solutions, it can be seem that the urea carbonyl oxygen has a preference over the urea nitrogen in binding to the peptide backbone during the last 5 ns (Fig. 10). This is in agreement with the previously interpretation provided by Hua et al. [19] that the binding of the urea oxygen to the backbone amide proton is the primary mechanism by which urea disrupts the folded structure. On the other hand, the strength of the interaction between water oxygen and the amide nitrogen slightly increases with time (Fig. 10). This finding shows that water solvate the peptide backbone slightly better at the end of the simulation (Last 5 ns), when the native structure is unfolded.

Potential mean force

Here, we used the same procedure as done by previous studies [1, 36] to calculate PMFs of the C_β of hydrophobic residues. This procedure occurred for both aqueous urea and GdmCl solutions. Figure 11a shows a clearly defined contact minimum (CM) for different concentrations of urea and pure water solution. In all solutions, the positions of the minima (0.4–0.6 nm) remain the same while the depth of the minima increases in urea solutions. Our results

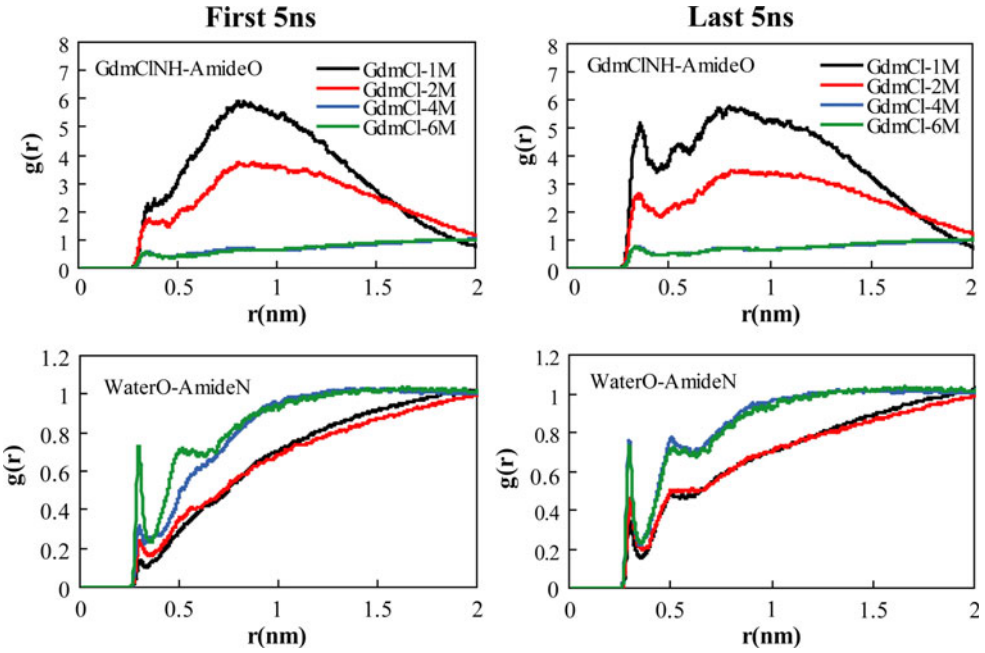

Fig. 9 Radial distribution functions between the oxygen atoms on the backbone and the nitrogen atoms on the GdmCl molecules and the oxygen atoms on the water and the nitrogen atoms on the backbone at various concentrations of GdmCl

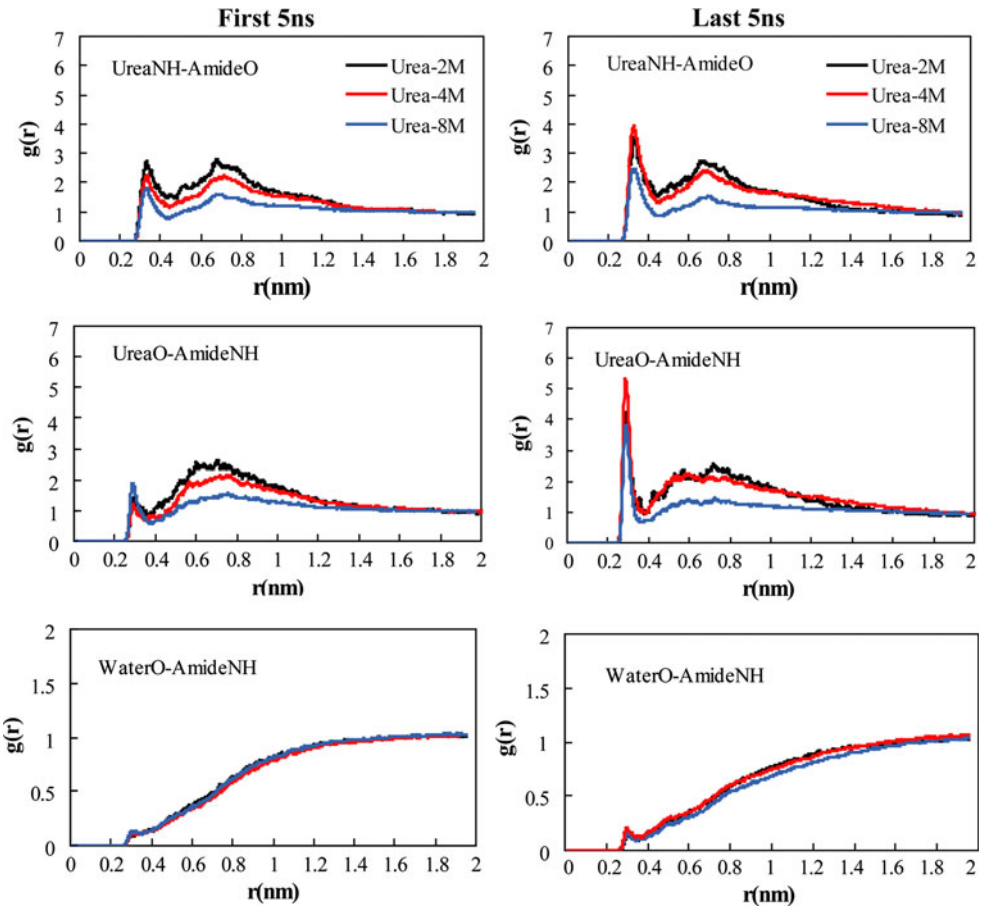

Fig. 10 Radial distribution functions between the oxygen atom on the bacbone and the nitrogen atoms on the urea, the oxygen atom on the urea and the nitrogen atoms on the backbone, and the oxygen atoms on the water and the nitrogen atoms on the backbone at various concentrations of urea

indicate a stabilization of hydrophobic residues in urea compared to that in water solution. The depth of the contact minimum (CM) increases as urea decreases (Fig. 11a). This means that hydrophobic residues are in more favorable environment in 2 M urea solution than 8 M urea.

The PMF of hydrophobic residues in GdmCl solutions show that the position of the CM (0.4–0.6 nm) are approximately the same at all GdmCl concentrations, however, the minima is deeper in low concentrations (Fig. 11b). The depth of the minima also increases at the CM by 0.3 and 0.1 kcal/mol in 1 and 2 M GdmCl compared to pure water, respectively. This study shows that the minima of the PMF in 1 M GdmCl are deeper before 25 ns (0–25 ns) than after that (25–40 ns) at the CM by approximately 0.4 kcal/mol (Fig. 11c). Comparison of the contact minimum of the hydrophobic residues between aqueous urea and GdmCl solutions shows that the depth of the minima in 2 and 4 M urea is more with respect to the same concentrations of GdmCl (Fig. 11a,b).

Discussion

Protein and peptide stability depends on a balance between the intramolecular protein–protein interactions and their interactions with the solvent environments. Adding osmolytes into the protein solution can modify this balance. Therefore, the solvent and co solvents play a central role in the non-covalent interactions responsible for the unique 3D structures of native proteins. Previous studies [10–20, 38] have shown that there are some models for protein denaturation by the denaturing osmolytes. In the first model, the denaturing molecules interact directly with protein, and in the second model, the effects are indirect. In the third model, there is a combination of direct and indirect effects. In the present study, we used comparative MD simulations to observe the denaturation mechanisms by GdmCl and urea at the atomic level details. The analyses were done from all three independent trajectories and the reported results contain analysis from one of the three trajectories. Thus, by showing the mechanisms of GdmCl and urea denaturation of the peptide in the simulations, we will able to elucidate which of the three interaction models drives denaturant-induced unfolding. The MD simulations in urea and GdmCl solutions are compared with simulations performed in TFE/water mixture and pure water in order to discriminate the net effect of the osmolyte denaturants. Together with previous studies [39–43], our results also reveal that magainin 2 is in an unstructured conformation in equilibrium with random coil structures in pure water,

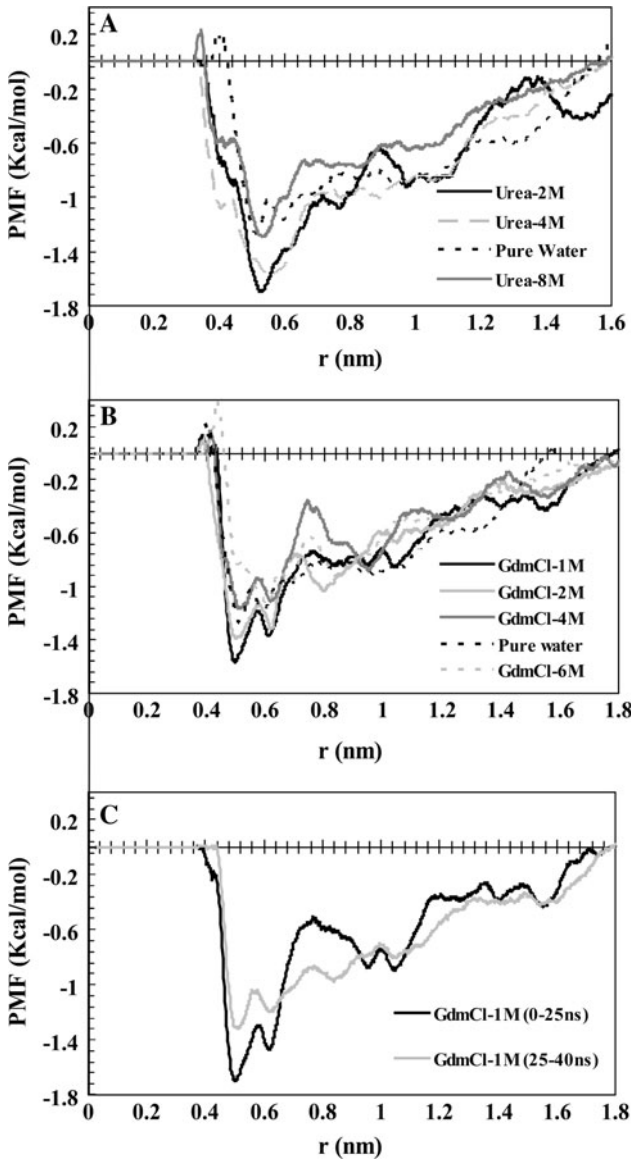

Fig. 11 Potential of mean force (PMF) the C_β of hydrophobic residues obtained from urea and GdmCl simulations of magainin

but obtains helical conformation when settled in TFE/water solution supported by previous works. In contrast to TFE, urea is known to induce helix unfolding in related alanine based peptides [44, 45]. Tanford was the first to study quantitatively the unfolding of proteins by urea [46]. He has shown that when a protein unfolds many peptide groups and non-polar side chains that were buried in the folded protein are exposed to solvent in the unfolded state. We now have a good understanding of how urea denatures proteins because of careful studies and thoughtful analyses from previous reports [15, 47–54]. Studies by Timasheff [53] and Record [49] have shown that urea binds preferentially to peptides over water, so the concentration of urea near the peptide is greater than the concentration in the bulk solvent. Thus, as the urea concentration increases, the denatured state will be favored because it has a much greater surface to interact with the urea. Mukhopadhyay and coworkers [1] have reported that the urea-induced denaturation can involve four steps: (a) breaking of the water structure by urea; (b) removal of the water solvation shell from peptide surface; (c) formation of strong hydrogen bonds with polar groups of peptides; (d) potential ability of urea molecules to form hydrogen bonds simultaneously with multiple amino acid residues, which in turn can adjust the local structures. In this study, we hypothetically divide these steps in two distinct phases, an indirect phase involves steps (a) and (b), and a direct phase involves steps (c) and (d). According to this hypothesis, the indirect phase produces more hydrophobic environment in solvation shell around the protein by removal of water molecules from protein surface and urea molecules stabilize hydrophobic residues. For proteins that are stable in aqueous solution, these phases induce protein unfolding through influence on hydrophobic force and direct interactions with protein backbone [10–20].For membranous proteins that are more stable in hydrophobic environment compared to aqueous solution, the indirect phase of urea action could stabilize protein structure while the direct phase induces denaturation. Study of membranous peptides in low urea concentrations seems to help to examine accuracy of this model. Because, the peptide denaturation in high concentration of urea occurs very fast and so monitoring of the early stages of the denaturation is difficult. The present study shows that the alpha helical structure of the peptide in water simulation is disappeared after 5 ns while the helicity of peptide is disappeared after 70 ns in 2 M (see supplementary Figs. 12 and 13) and 35 and 23 ns, in 4 M and 8 M urea simulations, respectively. Surprisingly, this result shows that the alpha helical structure of magainin in low aqueous urea solutions is remained more with respect to that solvated in pure water. To check this trend, the contact coefficient for all residues and potential mean force of hydrophobic residues were calculated [55]. Accordingly, urea interacts preferentially to the aromatic and non-polar side chains particularly in low concentrations and position of the contact minimum (CM) for the hydrophobic residues remains the same in all solutions while the depth of the minima increases in urea solutions. The depth of the minima also increases as urea concentration decreases. Therefore, accumulation of urea molecules in low concentration near hydrophobic residues provides environments that are more favorable which delays denaturation, pointing to the indirect effect of urea. On the other hand, direct interactions with the peptide begin to dominate in high urea solutions. The urea molecules can efficiently form hydrogen bonds with water as well as with other species such as the peptide backbone or charged hydrophilic side chain. This ability is the primary reason that

water structure is unperturbed even in high urea concentrations [15, 36]. Here, we find that hydrogen bond interactions between urea molecules and the peptide backbone are the dominant mechanism by which the peptide is unfolded in high urea concentrations. The urea molecules interact strongly with the peptide backbone and are absorb onto hydrophilic charged residues situated at the surface of the peptide. This leads to the swelling of the peptide, the exposure of hydrophobic residues, and eventually to the penetration of water and denaturant into the core of the peptide. These results lead us to the direct interaction mechanism in urea mediated peptide denaturation [10–15]. In overall, it can be concluded that urea have both the indirect and the direct effects but in high concentrations, the direct interaction is dominant.

Magainin approximately shows the same behavior in aqueous GdmCl solutions. Our study shows that the alpha helical structure of magainin in 1 M and 2 M GdmCl simulations is remained more than pure water (Fig. 2). GdmCl molecules, especially in 1 M and 2 M GdmCl solutions, tend to engage in transient stacking interactions with planar π-systems of aromatics side chains which lead to displacement of water from the hydration surface (Fig. 6b), providing more favorable environment for aromatic and other hydrophobic planar side chains. Intensity of the g(r) peaks obtained from pair correlation function between water oxygen and backbone amide hydrogen shows that water molecules are less ordered around the neighborhood of the protein backbone in 1 and 2 M GdmCl in compare to 4 and 6 M GdmCl (Fig. 9). This indicates that accumulation of GdmCl near hydrophobic surfaces in low GdmCl solutions prevents proper solvation of the peptide at the beginning. The PMFs of the hydrophobic residues in GdmCl solutions also show a clearly defined contact minimum (CM), a desolvation barrier, and a solvent separated minimum (SSM) (Fig. 11b). The depth of the contact minimum (CM) increases as GdmCl decreases. At low GdmCl concentrations, the desolvation barrier increases. These results confirm that water molecules solvate the peptide in pure water, 4 and 6 M GdmCl better than 1 and 2 M GdmCl. The poor solvation of magainin by water molecules keeps its alpha helical structure for 25 ns in 1 M GdmCl. Figure 11c shows that the depth of the minima and the desolvation barrier in 1 M GdmCl decreases after 25 ns. Therefore, the peptide can be solvated better by water causing completely disappearance of the peptide helicity after 25 ns. This work strongly suggests that hydrogen bonds between the peptide and water are important factors in the destabilization of peptide in aqueous GdmCl solutions. Our simulations also show that GdmCl to be more efficient than urea in denaturing magainin that is in agreement with experiment by Lim et al. [56] that GdmCl can be up to 4-fold more efficient than urea when planar amino acid side chains are major contributors to helical stability.

Acknowledgments The support of the Azarbaijan University of Tarbiat Moallem is gratefully acknowledged.

References

1. Das A, Mukhopadhyay C (2008) J Phys Chem B 112:7903–7908
2. Dill KA (1990) Biochemistry 29:7133–7155
3. Tanford C (1968) Adv Protein Chem 23:121–282
4. Tanford C, Kawahara K, Lapanje S (1966) J Biol Chem 241:1921–1923
5. Greene RF, Pace CN (1974) J Biol Chem 249:5388–5393
6. Arakawa T, Timasheff SN (1984) Biochemistry 23:5924–5929
7. Mehrnejad F, Naderi-Manesh H, Ranjbar B (2007) Proteins 67:931–940
8. Mehrnejad F, Chaparzadeh N (2008) J Biomol Struct Dyn 26: 255–262
9. Möglich A, Krieger F, Kiefhaber T (2005) J Mol Biol 345: 153–162
10. Shellman JA (1955) Comp Rev Trav Lab Carlsberg 29:223–229
11. Kresheck GC, Scheraga HA (1965) J Phys Chem 69:1704–1706
12. Frank HS, Franks F (1968) J Chem Phys 48:4746–4757
13. Wallqvist A, Covell DG, Thirumalai D (1998) J Am Chem Soc 120:427–428
14. Tobi D, Elber R, Thirumalai D (2003) Biopolymers 68:359–369
15. Bennion BJ, Daggett V (2003) Proc Natl Acad Sci USA 100: 5142–5147
16. Zou Q, Habermann-Rottinghaus SM, Murphy KP (1998) Proteins 31:107–115
17. Camilloni C, Rocco AG, Eberini I, Gianazza E, Broglia RA, Tiana G (2008) Biophys J 94:4654–4661
18. Stumpe MC, Grubmüller H (2008) PLoS Comput Biol 4:e1000221
19. Hua L, Zhou R, Thirumalai D, Berne BJ (2008) Proc Natl Acad Sci USA 105:16928–16933
20. Mason PE, Brady JW, Neilson GW, Dempsey CE (2007) Biophys J 93:L04–L06
21. Gesell J, Zasloff M, Opella SJ (1997) J Biomol NMR 9:127–135
22. Grant E, Beeler TJ, Taylor KM, Gable K, Roseman MA (1992) Biochemistry 31:9912–9918
23. Sheynis T, Sykora J, Benda A, Kolusheva S, Hof M, Jelinek R (2003) Eur J Biochem 270:4478–4487
24. Kandasamy SK, Larson RG (2004) Chem Phys Lipids 132: 113–132
25. Berendsen HJC, van der Spoel DJ, van Drunen R (1995) Comp Phys Comm 91:43–56
26. Lindahl E, Hess B, van der Spoel D (2001) J Mol Mod 7:306–317
27. Van Gunsteren WF, Billeter SR, Eising AA, Hünenberger PH, Krüger P, Mark AE, Scott WRP, Tironi IG (1996) Hochschulverlag AG an der ETH Zürich, Zürich
28. Van der Spoel D, van Buuren AR, Apol E, Meulenhoff PJ, Tieleman DP, Sijbers ALTM, Hess B, Feenstra KA, Lindahl E, van Drunen R, Berendsen HJC (2002) Department of Biophysical Chemistry. University of Groningen, Groningen
29. Berendsen HJC, Grigera JR, Straatsma TP (1987) J Phys Chem 91:6269–6271
30. Smith LJ, Berendsen HJC, van Gunsteren WF (2004) J Phys Chem B 108:1065–1071
31. Fioroni M, Burger K, Mark AE, Roccatano D (2000) J Phys Chem B 104:12347–12354

32. Darden T, York D, Pedersen LG (1993) J Chem Phys 98:10089–10092
33. Berendsen HJC, Postma JPM, van Gunsteren WF, Di Nola A, Haak JR (1984) J Chem Phys 81:3684–3690
34. Hess B, Bekker H, Berendsen HJC, Fraaije JGEM (1997) J Comput Chem 18:1463–1472
35. Stumpe MC, Grubmüller H (2007) J Am Chem Soc 129:16126–16131
36. O'Brien EP, Dima RI, Brooks B, Thirumalai D (2007) J Am Chem Soc 129:7346–7353
37. Kabsch W, Sander C (1983) Biopolymers 22:2577–2637
38. Robinson DR, Jencks WP (1965) J Am Chem Soc 87:2462–2469
39. Roccatano D, Colombo G, Fioroni M, Mark AE (2002) Proc Natl Acad Sci USA 99:12179–12184
40. Kumar S, Modig K, Halle B (2003) Biochemistry 42: 13708–13716
41. Gerig JT (2004) Biophys J 86:3166–3175
42. Roccatano D, Fioroni M, Zacharias M, Colombo G (2005) Protein Sci 14:2582–2589
43. Chatterjee C, Gerig JT (2006) Biochemistry 45:14665–14674
44. Smith JS, Scholtz JM (1996) Biochemistry 35:7292–7297
45. Scholtz JM, Barrick D, York EJ, Stewart JM, Baldwin RL (1995) Proc Natl Acad Sci USA 92:185–189
46. Tanford C (1964) J Am Chem Soc 86:2050–2059
47. Tsai J, Gerstein M, Levitt M (1996) J Chem Phys 104:9417–9430
48. Tirado-Rives J, Orozco M, Jorgensen WL (1997) Biochemistry 36:7313–7329
49. Courtenay ES, Capp MW, Saecker RM, Record MT (2000) Proteins 4:72–85
50. Zou Q, Bennion BJ, Daggett V, Murphy KP (2002) J Am Chem Soc 124:1192–1202
51. Soper AK, Castner EW, Luzar A (2003) Biophys Chem 105:649–666
52. Modig K, Kurian E, Prendergast G, Halle B (2003) Protein Sci 12:2768–2781
53. Timasheff SN, Xie G (2003) Biophys Chem 105:421–448
54. Schellman JA (2003) Biophys J 85:108–125
55. van der Vegt NF, Lee ME, Trzesniak D, van Gunsteren WF (2006) J Phys Chem B 110:2852–12855
56. Lim WK, Rösgen J, Englander SW (2009) Proc Natl Acad Sci USA 106:2595–2600